

Fe⁰/PTFE Triboelectric Nanogenerators for Ultrafast Dye and Antibiotic Degradation

Xiao-Feng Xu, Zhao-Jian Li, Zhen Zhang, Shuai-Yu Wu, Kai-Zhen Yuan, Lu-Yao Wang, Yun-Ze Long,* and Hong-Di Zhang*



Cite This: *ACS Omega* 2025, 10, 12233–12240



Read Online

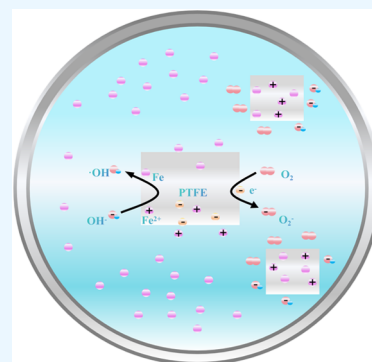
ACCESS |

Metrics & More

Article Recommendations

Supporting Information

ABSTRACT: Triboelectric catalysis is a new technology that converts mechanical energy to chemical energy. This study presents a novel efficient triboelectric catalytic design based on iron (Fe⁰) and polytetrafluoroethylene (PTFE). The tribocatalytic effect was evaluated by degrading methyl orange (MO), crystal violet (CV), and tetracycline (TC). The degradation efficiency can reach 95, 97, and 93% within 24 min, respectively, and the kinetic constant *K* of CV was as high as 0.1460 min⁻¹. The comparison with the stirring experiment showed that the friction catalytic effect between Fe⁰ and PTFE was significantly enhanced under ultrasonic irradiation. Furthermore, the triboelectric effect is used to provide simplicity and strong triboelectric catalytic activity of Fe⁰/PTFE, and the influencing factors are analyzed. And the production of reactive oxygen species (ROS) of hydroxyl radicals and superoxide radicals increases during the catalytic process. The mechanism of triboelectric catalysis is discussed in terms of electron transfer and transition. This study utilizes the triboelectric effect of Fe⁰/PTFE to provide simplicity and superior triboelectric catalytic activity under ultrasonic irradiation.



1. INTRODUCTION

With the continuous development of industry, textile, pharmaceutical, and other industries produce a large amount of industrial wastewater, so the environment is facing serious challenges.¹ Azo dyes are widely used in the textile industry, and about 10–15% of the dyes are discharged into the environment without treatment during the production process, causing damage to the environment and affecting people's lives. Antibiotics are widely used in medicine, and it is inevitable that they will flow into the environment during use. TC accounts for a very high proportion of wastewater monitoring. With the development of industry, traditional wastewater treatment methods have shown obvious disadvantages. For example, physical adsorption can only achieve the transfer of dyes and other molecules and cannot fundamentally eliminate;² Biological decomposition efficiency is slow;³ Chemical oxidation energy consumption is huge;⁴ the study of efficient and stable wastewater treatment methods has become an important issue of environmental protection. In 2012, Wang et al. first proposed the friction nanogenerator (TENG),⁵ the principle of which is to convert mechanical energy into electrical energy through triboelectric effect and electrostatic induction to achieve self-power supply, making great contributions to energy saving and environmental protection.⁶ After the study of others, the solid–solid friction, solid–liquid friction, and other systems can be used for catalytic degradation and environmental protection.^{7–9}

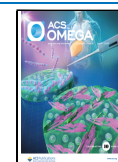
Triboelectric catalysis refers to the triboelectric effect generated by mechanical energy to drive the catalytic effect.^{10,11} Triboelectric catalysis is an emerging catalytic effect that collects mechanical energy from the environment, such as collisions and vibrations, to enable self-powering chemical reactions. In recent years, TENG has made extensive research and progress in the fields of sensing and medical sterilization.^{12–14} The combination of mechanical luminescence and TENG generates power through mechanical operation and provides important visual input in the form of light emission, enabling sensitive detection of motion signals; the TENG provides a stable electric field for sterilization devices, attracting microorganisms into the local electric field area and effectively inactivating them through electroporation. However, there is a problem of low efficiency in its application in the field of water purification, and improving its efficiency will be the focus of research in the field of water purification. Compared with photocatalysts which require a special band gap, and piezoelectric catalysts which require an asymmetric center structure,^{15,16} triboelectric catalysis has a wider range of materials, including traditional polymers such as polytetra-

Received: December 1, 2024

Revised: February 22, 2025

Accepted: March 5, 2025

Published: March 17, 2025



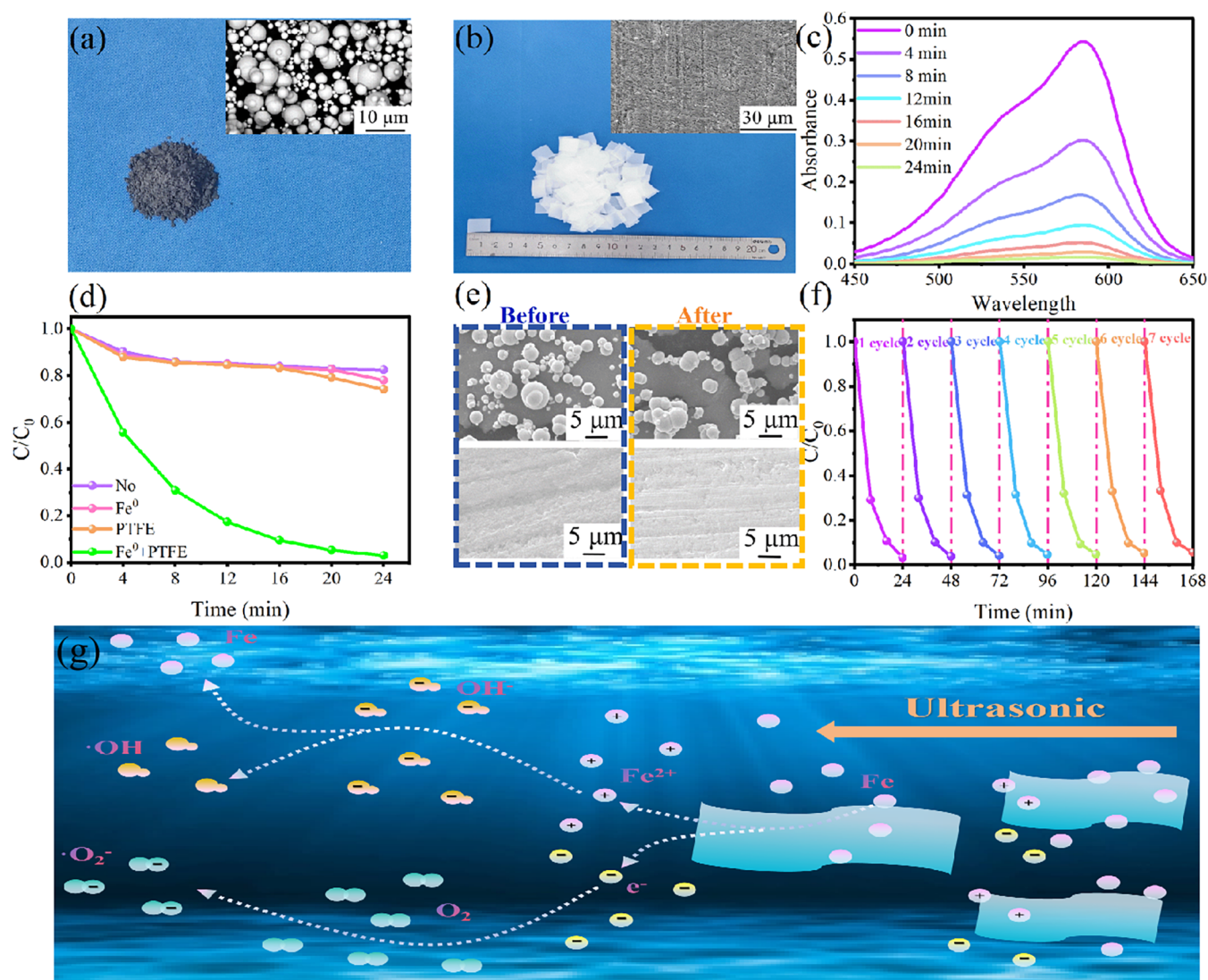


Figure 1. (a) Fe⁰ optical image and SEM; (b) PTFE optical images and SEM; (c) ultrasonic catalytic degradation of CV; (d) comparison of degradation of different drug additives; (e) Fe⁰/PTFE degradation test before and after comparison; (f) cyclic experiment; (g) simulation diagram of frictional electrocatalysis.

fluoroethylene (PTFE)¹⁵ and fluorinated ethylpropylene (FEP),¹⁷ semiconductor catalysts,¹⁸ and metals.¹⁹ Solid–solid friction is limited by stirring as the friction driving force; therefore, it is difficult to produce efficient friction and it is difficult to produce efficient triboelectric catalysis. Polytetrafluoroethylene (PTFE) is a kind of composite material with high electronegativity and acid-alkali resistance,^{20,21} has a broad application prospect in the field of anticorrosion and triboelectric power generation, and is an ideal triboelectric catalytic material. Studies have shown that ZnO nanorods with PTFE can reduce the degradation rate of Rhodamine B by 99% under the condition of 1000 rpm magnetic stirring for 60 h.¹⁸ Using PTFE particles (1–5 μm) as catalyst, the degradation efficiency of PFAS (perfluorinated and polyfluoroalkyl substances) reached 90% within 120 min.²² PTFE is inert and extremely electronegative, but most of the existing research has focused on its frictional action with water molecules^{23–25} or its piezoelectric catalysis.^{26,27} We assume that the selection of materials with low electronegativity, such as active metal elements, friction with PTFE will easily generate electron transfer between them, and if more efficient

friction conditions can be created, it will be a major breakthrough in the triboelectric catalysis of PTFE.

2. EXPERIMENTAL SECTION

2.1. Material. Micron grade industrial iron powder, purchased from Guangzhou Metal Metallurgy Co., Ltd.; polytetrafluoroethylene (PTFE), purchased from Shanghai Aladdin Biochemical Technology Co., Ltd.; Crystal violet (CV), Methyl orange (MO), and tetracycline (TC), purchased from Shanghai Macklin Biochemical Co., Ltd.; hydroxylamine hydrochloride, purchased from Tianjin Damao Chemical Reagent Factory; phenanthroline, purchased from Shandong Xiya Chemical Co., Ltd.

2.2. Method. In this study, a novel and efficient triboelectrocatalytic design is proposed. PTFE has extremely high electronegativity, is easy to obtain electrons, and also has hydrophobicity. In order to achieve a better friction effect in the experiment, we chose a thin film as the experimental material. Fe, as an active metal, is easy to prepare and obtain at a low cost; stable during the ultrasound experiment, easy to recover after the experiment, and will not cause secondary

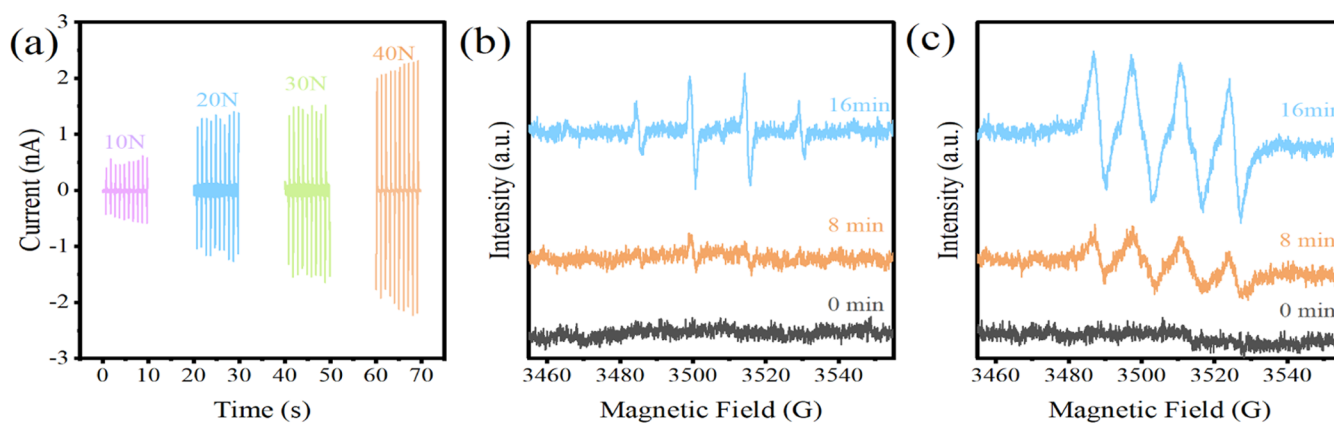


Figure 2. (a) Triboelectric test diagram of Fe⁰ and PTFE; EPR tests for (b) •OH and (c) •O₂⁻.

pollution to the water. In the experiment, a 0.2 g (1–1.5 cm long and wide, 0.0127 cm thick) PTFE film and 20 mg iron particles are used, and the PTFE film is pressed to the bottom by water pressure, which makes friction in aqueous solution possible. Add 10 mL of 5 mg L⁻¹ dye solution into the vial. The experiment was carried out under ultrasonic conditions with a frequency of 20 kHz and power of 600 W, and the degradation of MO, CV, and TC was highly efficient. The triboelectric catalytic effect was demonstrated by adding Fe⁰ and PTFE, respectively, and its stability was proved by cyclic experiment. The self-assembled triboelectric test instrument is used for triboelectric and charge transfer test. The instrument is divided into two ends: one end is fixed, PTFE is placed on it, and Fe is placed on the other end. The collision friction between the two ends is driven by mechanical force, and the current or charge transfer is displayed in the oscilloscope. Electron spin resonance (EPR) was used to study reactive oxygen species (ROS).^{28–31} The degradation experiments were carried out under light and dark, stirring and ultrasonic, and different power conditions, to explore the limitations of light, temperature, and power on this frictional catalysis, the influencing factors of friction catalysis between Fe⁰ and PTFE were explored, and the principle of microcosmic analysis was carried out.

2.3. Characterization of Catalysts. Ultrasonic cell crusher provides ultrasonic conditions, output power 100–1000 W, and output frequency 20 kHz. Scanning electron microscopy (SEM) observations were conducted on a ZEISS Sigma 300 instrument. An ultraviolet (UV)-2700 UV–visible spectrophotometer (Shimadzu, Japan) was used to measure the UV–visible diffuse reflectance spectrum of samples, with barium sulfate as a reference, and the test range was 200–800 nm. Furthermore, the existence of ROS was also characterized using electron paramagnetic resonance (EPR, Bruker EMX-plus). Triboelectric testing for current and charge is recorded using a DSOX3024T digital storage oscilloscope (200 MHz 5GSa/s).

3. RESULTS AND DISCUSSION

3.1. Fe⁰/PTFE Ultrasonic Degradation of CV. Figure 1a,b shows the optical images and SEM of Fe⁰ and PTFE. It can be seen that the size of iron is mostly 1–5 μm, and the length and width of PTFE are 1–1.5 cm.

The ultrasonication makes the iron powder carry out Brownian movement in the solution, makes the PTFE slightly shake at the bottom of the solution, and the Fe⁰ and PTFE

produce friction in the solution, the transfer of charge occurs, and then reactive oxygen species (ROS) is produced, to achieve the effect of degrading molecules such as dyes. Figure 1c shows the absorbance test diagram of 5 mg L⁻¹ CV solution degraded at different times. The degradation rate of CV was 69% when degraded for 8 min. The degradation rate of CV was 90% after 16 min degradation. When the degradation time reaches 24 min, the degradation rate of CV reaches 97%.

In order to verify the frictional catalytic effect of Fe⁰ and PTFE, experiments were carried out to add drugs separately. Figure 1d shows the comparison of degradation of different drugs, and the absorbance degradation diagram with a time gradient of 4 min is shown in SM Figure S1. It can be seen that the degradation rate of CV was 14, 16, and 18% within 8, 16, and 24 min, respectively, under ultrasonic irradiation, which may be the catalytic effect of ultrasonic oxidation of water to H₂O₂.³² After adding PTFE into CV solution, the degradation rate was 14, 17, and 26% at 8, 16, and 24 min, respectively. It has been reported that ultrasound can activate PTFE so that it has a piezoelectric catalytic effect,²⁵ which is not obvious from Figure 1d probably because of the short time. Fe⁰ was added into CV solution, and the degradation rate was 14, 17, and 22% after 8, 16, and 24 min, respectively, which may be due to the electrofenton effect of iron, generating hydroxyl free radicals, resulting in catalytic degradation.³³ After adding Fe⁰ and PTFE into CV solution, the degradation rate was 69, 90, and 97% at 8, 16, and 24 min, respectively. Compared to the experiments mentioned above, the degradation efficiency of CV is greatly improved, and a high degree of degradation is achieved in a short time, indicating that there is a high degree of triboelectric effect between Fe⁰ and PTFE. In order to verify the triboelectric catalytic stability of Fe⁰ and PTFE, repeated experiments were carried out. Figure 1e shows the SEM comparison of Fe⁰/PTFE before and after a degradation experiment. It can be seen that the microscopic morphology has no obvious change. Figure 1f shows the degradation experiment diagram of seven cycles, and the detailed absorbance test diagram of different cycles is shown in Supporting Figure S2. As can be seen from the figure, the degradation rate of the first cycle is 97%. The second cycle degradation rate was 96%. The third cycle degradation rate was 96%. The fourth cycle degradation rate was 95%. At the fifth cycle, 95% degradation can still be achieved, indicating that the friction catalysis of Fe⁰ and PTFE has good stability. Figure 1g is a simulation diagram of the entire experimental process

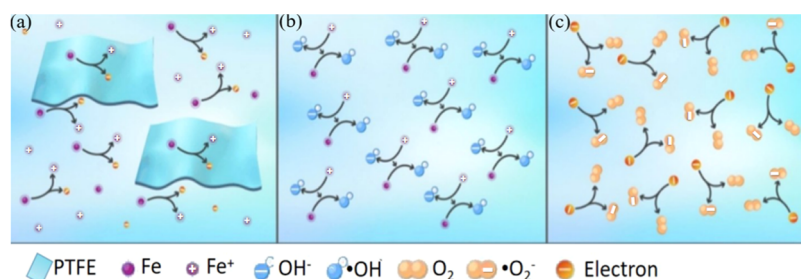


Figure 3. (a) Friction between PTFE and Fe^0 ; (b) Fe^{2+} form $\bullet\text{OH}$ with OH^- ; (c) electrons form $\bullet\text{O}_2^-$ with O_2 .

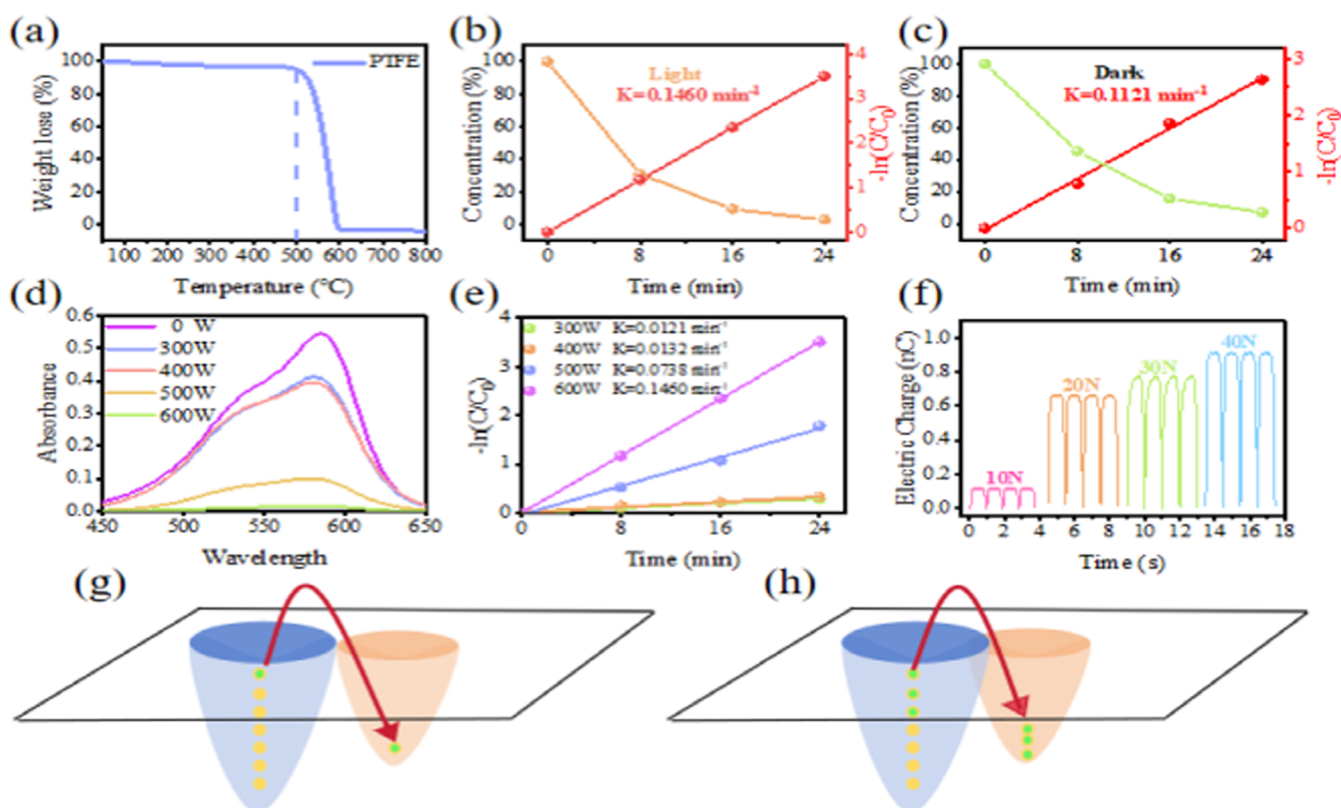


Figure 4. (a) PTFE thermogravimetric test; (b) light degradation curve and kinetic constant; (c) dark degradation curve and kinetic constants; (d) CV degradation absorbance curve at different power levels for 24 min; (e) K values at different power; (f) charge transfer under different pressures; (g) charge transfer between electron clouds at Weak friction force; (h) charge transfer between electron clouds at Strong friction force.

3.2. Principle Analysis of Fe^0 /PTFE Triboelectric Catalysis. In order to characterize the friction principle between Fe^0 and PTFE, triboelectric simulation tests were carried out, as shown in Figure 2a. Because Fe^0 and PTFE produce frictions similar to collisions in solution, extruded triboelectric experiments were carried out under different pressures. It can be seen that the current generated by friction increases with an increase of the friction driving force. The friction mechanism was analyzed from the perspective of microscopic ROS. The EPR test is shown in Figure 2b–c. It can be seen that the production of ROS increases with time. The strong signals of the hydroxyl radical and superoxide radical were detected, indicating that the combined action of the hydroxyl radical and superoxide radical induced triboelectric catalysis.

Combined with the above experimental results, a possible friction model was simulated: in the ultrasonic experiment, the iron particles were uniformly distributed and moved irregularly in the solution, while the PTFE moved slightly at the bottom

of the solution. The friction model is shown in Figure 3a. Iron particles and PTFE produce friction similar to collisions. Electron transfer and electron transition are the main factors of triboelectricity, the principle of electron transfer is the electron transfer between atoms,³⁴ that is, the mechanical force causes the friction between the catalyst and the surrounding solid or liquid environment so as to achieve electron transfer directly involved in the transfer of chemical reactions to achieve friction catalysis,³⁵ and materials that gain or lose electrons contribute to the production of active substances that participate in the next redox reaction. Electron transfer can cause electron transitions, which occur when the electrons gained or lost by the catalyst are stimulated by mechanical or thermal energy. During the friction process, iron particles lose electrons, while polytetrafluoroethylene gains electrons and reacts with OH^- and O_2 in water to form $\bullet\text{OH}$ and $\bullet\text{O}_2^-$ respectively, as shown in Figure 3b–c. Hydroxyl radicals and superoxide radicals work together to degrade dye molecules in water. To investigate possible reactions, Fe^{2+} concentration

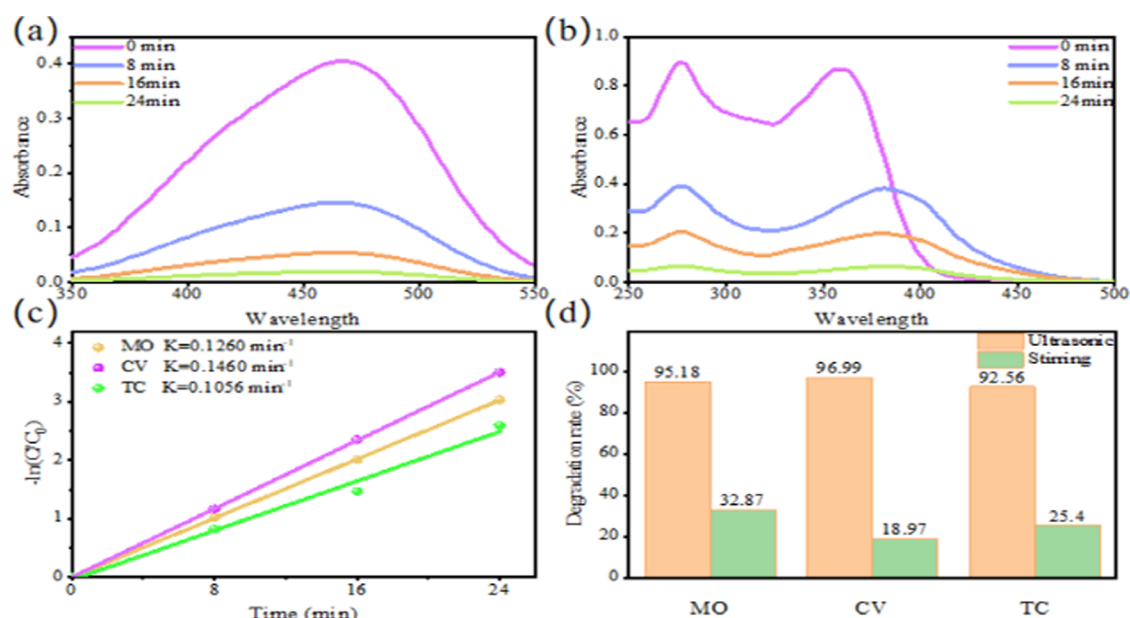
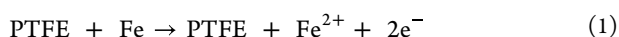


Figure 5. (a) Degradation curve of MO; (b) degradation curve of TC; (c) K value of MO, CV, and TC degradation; (d) comparison of stirring and ultrasonic degradation.

tests were performed, by setting 10 mg/L FeSO_4 solution as the standard solution, experimental samples with ultrasonic duration of 4, 8, 12, 16, 20, and 24 min are respectively added with phenanthroline solution for staining, and absorbance test is performed. The Fe^{2+} concentration of each time period was obtained by the ratio of wave peak size, and the data are supplemented in Figure S3. The possible reaction mechanism of the whole process is shown in the following equation:



Under the action of ultrasound, Fe undergoes irregular motion in water, while the PTFE film vibrates slightly in water. When Fe comes into contact with PTFE, the electron clouds overlap. Due to PTFE's high electronegativity, active electrons are induced to undergo transitions, generating superoxide radicals with O_2 in water; Positively charged Fe^{2+} reacts with $-\text{OH}$ in water to generate hydroxyl radicals. Two types of reactive oxygen species catalyze the degradation of the dye molecules in water.

3.3. Analysis of Influencing Factors of Fe^0/PTFE Triboelectric Catalysis. Industrial wastewater is usually accompanied by a certain temperature; in order to explore the possibility of working in a high-temperature environment, we conducted a thermogravimetric test of PTFE, and the results are shown in Figure 4a. It can be seen from Figure 4a that PTFE can remain stable when it is less than 500 °C, and PTFE is decomposed by heat when it is higher than 500 °C. The temperature of industrial wastewater is usually 40 °C. We conducted experiments under different temperature conditions, and the experimental results at 30, 40, 50, and 60 °C are provided in Supporting Figure S6. It was found that different temperatures had no effect on the catalytic experiment. Therefore, Fe^0/PTFE can be triboelectrically catalyzed at

high temperatures. The experimental comparison between light and dark environments was carried out, and the test results are shown in Figure 4b,c. Under the condition of light, the degradation rate of CV solution was 69% in 8 min. The degradation rate in 16 min was 90%. The degradation rate of 97% can be achieved in 24 min, and the rate constant is $K = 0.1460 \text{ min}^{-1}$. Under dark conditions, the degradation rate was 55% after 8 min. The degradation rate was 84% after 16 min. The degradation rate of 93% can be achieved in 24 min, and the rate constant $K = 0.1121 \text{ min}^{-1}$. It can be seen that there is no significant difference in the degradation rate between light and dark conditions, indicating that the presence of light does not limit the triboelectric catalysis of Fe^0/PTFE . From Figure 2a, we find that under different friction driving forces, the current generated increases with the increase of pressure, considering that ultrasonic power may be an important factor affecting triboelectro catalysis. A power control experiment was measured. The absorbance curve of CV solution under ultrasonic degradation for 24 min at different powers is shown in Figure 4d, and the detailed absorbance curve under different powers is shown in Supporting Figure S4.

At 300 W, the degradation rate of CV is 25%. At 400 W, the degradation rate of CV is 28%. At 500 W, the degradation rate of CV is 83%. At 600 W, the degradation rate of CV is 97%. The K value under different powers is shown in Figure 4e. Under 300 W power, $K = 0.012 \text{ min}^{-1}$; At 400 W, $K = 0.013 \text{ min}^{-1}$; At 500 W, $K = 0.073 \text{ min}^{-1}$; At 600 W, $K = 0.146 \text{ min}^{-1}$. When the power rises from 400 to 500 W, the triboelectric catalytic effect of Fe^0/PTFE is significantly improved. When the power is 300 or 400 W, Fe^0 is in a state of difficult movement, sinking at the bottom of the solution, PTFE has no macroscopic movement at the bottom of the solution, Fe^0 and PTFE are difficult to produce effective friction; When the power rose to 500 W, Fe^0 carried out Brownian movement in the solution, and when the power rose to 600 W, Fe^0 Brownian movement was more intense, and Fe^0/PTFE obviously had better friction effect under ultrasonic irradiation, resulting in a significant catalytic effect. With the

increase of ultrasonic power, the degradation rate of CV increased in 24 min. The reason may be that the charge transfer amount of Fe⁰ and PTFE is different under different powers, which affects the generation of ROS, and then affects the degradation efficiency of CV. An electron cloud potential trap model is introduced.³³ When two media are contacted by external forces, a local high pressure is generated at the point of contact, even on the atomic scale. As the acting force increases, the distance between atoms belonging to different media decreases, causing their electron clouds to overlap to increase, as shown in Figure 4g–h. This stronger electron cloud overlap is thought to lower the energy barrier for electron exchange. Therefore, when the friction process is subjected to higher contact forces, more electrons will be transferred. In order to verify the conjecture, charge transfer tests were carried out under different pressures, and the test results are shown in Figure 4f. Under the pressure of 10 N, the charge transfer is 0.11 nC. Under the pressure of 20 N, the charge transfer is 0.66 nC. Under the pressure of 30 N, the charge transfer is 0.77 nC. At a pressure of 40 N, the charge transfer is 0.91 nC. As the pressure increases, the amount of charge transfer gradually increases. This is consistent with the result that the degradation rate of CV increases with the increase of ultrasonic power. The reason may be that the Strong friction force can cause a high degree of overlap of the electron cloud, which is more conducive to the transfer of electrons. We drew a simulation diagram, as shown in Figure 4g–h. At Weak friction force, as shown in Figure 4g, the electron cloud contacts and transfers a small amount of charge; At strong friction force, as shown in Figure 4h, the electron cloud has a high degree of overlap, which is more conducive to electron transfer and ROS generation, thus producing higher catalytic efficiency.

In order to study the applicability of Fe⁰/PTFE triboelectric catalysis, ultrasonic degradation experiments of MO and TC were conducted, and the degradation curves are shown in Figure 5a,b. The degradation rate of MO was 64% after 8 min ultrasound. The degradation rate was 87% after 16 min. The degradation rate was 95% after 24 min. The degradation rate of TC was 56% after 8 min of ultrasound. The degradation rate was 77% after 16 min. The degradation rate was 93% after 24 min. The fitted *K* values of MO, CV, and TC are shown in Figure 5c, where $K_{MO} = 0.126 \text{ min}^{-1}$, $K_{CV} = 0.146 \text{ min}^{-1}$, and $K_{TC} = 0.105 \text{ min}^{-1}$. The comparison of the triboelectric catalytic efficiency with relevant studies is shown in Table 1. The comparison of ultrasonic and agitation as friction driving forces was carried out; the test results are shown in Figure 5d, and the agitation degradation curve is shown in SM Figure S5. Because the ultrasonic process is accompanied by heat

generation, in order to ensure the uniqueness of the variables as much as possible, the stirring experiment was carried out under the condition of 50 °C water bath heating. At 24 min, the degradation rate of MO was 95% under ultrasonic condition, but only 33% under stirring condition. The degradation rate of CV was 97% under ultrasonic condition, but only 19% under stirring condition. The degradation rate of TC was 93% under ultrasonic condition, but only 25% under stirring condition. The results show that ultrasonics can provide better friction conditions for Fe⁰/PTFE. The reason is that stirring makes the iron powder and PTFE produce a single direction of movement, which makes the frequency of friction between Fe⁰ and PTFE greatly reduced, which greatly limits the friction between Fe⁰ and PTFE; The ultrasonic makes the iron powder carry out irregular movement in the solution, and the PTFE slightly vibrates at the bottom of the solution. Compared with stirring, ultrasonics increase the friction frequency of Fe⁰/PTFE, so the triboelectric catalytic effect is better.

4. CONCLUSIONS

In this article, solid–solid triboelectric catalysis between PTFE and Fe⁰ is designed for the first time. Within 24 min, the degradation rates of MO, CV, and TC solutions were all greater than 90%, and the CV rate constant *K* was as high as 0.146 min⁻¹. Triboelectric and EPR tests were carried out. The results showed that the friction between PTFE and Fe⁰ produced current and reactive oxygen species. The influence factors of triboelectric catalysis are studied. Temperature and light have no great limitations on triboelectric catalysis. The power will affect the overlap degree of electron cloud and then affect the efficiency of triboelectric catalysis. Compared with agitation, the triboelectric catalytic effect of Fe⁰ and PTFE was significantly enhanced under ultrasonic irradiation, indicating that the friction driving force is the key factor affecting the triboelectric catalytic effect. The mechanism of friction catalysis is discussed, with electron transfer and transition. This study utilizes the triboelectric effect to provide the simplicity and superior triboelectric catalytic activity of Fe⁰/PTFE.

■ ASSOCIATED CONTENT

Supporting Information

The Supporting Information is available free of charge at <https://pubs.acs.org/doi/10.1021/acsomega.4c10892>.

CV degradation curves under different conditions; CV degradation curves of five cycles; Fe²⁺ concentration test; CV degradation absorbance curve under different power; degradation curves of MO, CV, and TC under stirring conditions (PDF)

■ AUTHOR INFORMATION

Corresponding Authors

Yun-Ze Long – Collaborative Innovation Center for Nanomaterials & Devices, College of Physics, Qingdao University, Qingdao 266071, China; orcid.org/0000-0002-4278-4515; Email: yunze.long@qdu.edu.cn

Hong-Di Zhang – Collaborative Innovation Center for Nanomaterials & Devices, College of Physics, Qingdao University, Qingdao 266071, China; orcid.org/0000-0002-8240-8602; Email: zhanghongdi@qdu.edu.cn

Table 1. Comparison of the Degradation Efficiencies in Triboelectric Catalysis

frictional electrocatalysis	<i>K</i>
NiCo ₂ O ₄ frictional electrocatalytic degradation of Rhodamine B ³⁶	0.0762 h ⁻¹
ball milling PTFE degradation of MO ³⁷	0.0499 min ⁻¹
TENG and 3DGA@CDs-TNs photoelectric catalytic degradation of BG ³⁸	0.0536 min ⁻¹
TENG and 3DGA@CDs-TNs photoelectric catalytic degradation of DB ³⁸	0.0251 min ⁻¹
ultrasound Fe ⁰ /PTFE degradation of TC in this work	0.1059 min ⁻¹
ultrasound Fe ⁰ /PTFE degradation of MO in this work	0.1260 min ⁻¹
ultrasound Fe ⁰ /PTFE degradation of CV in this work	0.1460 min ⁻¹

Authors

Xiao-Feng Xu – Collaborative Innovation Center for Nanomaterials & Devices, College of Physics, Qingdao University, Qingdao 266071, China

Zhao-Jian Li – Department of Neurosurgery, Affiliated Hospital of Qingdao University, Qingdao 266003, China

Zhen Zhang – Collaborative Innovation Center for Nanomaterials & Devices, College of Physics, Qingdao University, Qingdao 266071, China

Shuai-Yu Wu – Collaborative Innovation Center for Nanomaterials & Devices, College of Physics, Qingdao University, Qingdao 266071, China

Kai-Zhen Yuan – Collaborative Innovation Center for Nanomaterials & Devices, College of Physics, Qingdao University, Qingdao 266071, China

Lu-Yao Wang – Collaborative Innovation Center for Nanomaterials & Devices, College of Physics, Qingdao University, Qingdao 266071, China

Complete contact information is available at:

<https://pubs.acs.org/10.1021/acsomega.4c10892>

Author Contributions

X.-F.X.: Writing—review and editing, writing—original draft, methodology, formal analysis, data curation. Z.-J.L.: Methodology, investigation, formal analysis, conceptualization. Z.Z.: Validation, software, investigation. S.-Y.W.: Writing—review and editing, supervision, conceptualization. K.-Z.Y.: Writing—review and editing, supervision, resources. L.-Y.W.: Validation, supervision, software, resources. Y.-Z.L.: Writing—review and editing, writing—original draft, funding acquisition, conceptualization. H.-D.Z.: Supervision, funding acquisition, conceptualization.

Notes

The authors declare no competing financial interest.

ACKNOWLEDGMENTS

This work was supported by the Shandong Provincial Natural Science Foundation, China (ZR2020MA066), the National Natural Science Foundation of China (52273077), and the State Key Laboratory of Bio-Fibers and Eco-Textiles, Qingdao University (ZDKT202108, RZ2000003334 and G2RC202022).

REFERENCES

- (1) Luo, Y. T.; Xie, K.; Peng, F.; Lavallais, C.; Peng, T.; Chen, Z.; Zhang, Z.; Wang, N.; Li, X. Y.; Grigioni, I.; Liu, B.; Sinton, D.; Dunn, J. B.; Sargent, E. H. Selective electrochemical synthesis of urea from nitrate and CO₂ via relay catalysis on hybrid catalysts. *Nat. Catal.* **2023**, *6*, 939–948.
- (2) Borodin, D.; Auerbach, D. J.; Zhong, T.; Guo, H.; Schwarzer, D.; Kitsopoulos, T. N.; Wodtke, A. M.; et al. Following the microscopic pathway to adsorption through chemisorption and physisorption wells. *Science* **2020**, *369*, 1461–1465.
- (3) Zhou, S.; Jia, Y.; Fang, H.; Jin, C.; Mo, Y.; Xiao, Z.; Zhang, N.; Sun, L.; Lu, H. A new understanding on the prerequisite of antibiotic biodegradation in wastewater treatment: Adhesive behavior between antibiotic-degrading bacteria and ciprofloxacin. *Water Res.* **2024**, *252*, No. 121226.
- (4) Amdouni, W.; Fricaudet, M.; Otonicar, M.; Garcia, V.; Fusil, S.; Kreisel, J.; Maghraoui-Meherzi, H.; Dkhil, B. BiFeO₃ nanoparticles: The “Holy-Grail” of piezo-photocatalysts. *Adv. Mater.* **2023**, *35*, No. 2301841.

(5) Wang, Z. L.; Zhu, G.; Yang, Y.; Wang, S.; Pan, C. Progress in nanogenerators for portable electronics. *Mater. Today* **2012**, *15*, 532–534.

(6) Cao, B.; Wang, P.; Rui, P.; Wei, X.; Wang, Z.; Yang, Y.; Tu, X.; Chen, C.; Wang, Z.; Yang, Z.; Jiang, T.; Cheng, J.; Wang, Z. Broadband and output-controllable triboelectric nanogenerator enabled by coupling swing-rotation switching mechanism with potential energy storage/release strategy for low-frequency mechanical energy harvesting. *Adv. Energy Mater.* **2022**, *12*, No. 2202627.

(7) Zhan, F.; Wang, A.; Xu, L.; Lin, S.; Shao, J.; Chen, X.; Wang, Z. Electron transfer as a liquid droplet contacting a polymer surface. *ACS Nano* **2020**, *14*, 17565–17573.

(8) Yang, P.; Shi, Y.; Tao, X.; Liu, Z.; Dong, X.; Wang, Z.; Chen, X. Radical anion transfer during contact electrification and its compensation for charge loss in triboelectric nanogenerator. *Matter* **2023**, *6*, 1295–1311.

(9) Wang, Z.; Berbille, A.; Feng, Y.; Li, S.; Zhu, L.; Tang, W.; Wang, Z. Contact-electro-catalysis for the degradation of organic pollutants using pristine dielectric powders. *Nat. Commun.* **2022**, *13*, No. 130.

(10) Fan, F.-R.; Xie, S.; Wang, G.; Tian, Z. Tribocatalysis: challenges and perspectives. *Sci. China: Chem.* **2021**, *64*, 1609–1613.

(11) Li, X.; Cao, N.; Zhang, T.; Fang, R.; Ren, Y.; Chen, X.; Bian, Z.; Li, H. Optimizing photocatalytic performance in an electrostatic-photocatalytic air purification system through integration of triboelectric nanogenerator and Tesla valve. *Nano Energy* **2024**, *128*, No. 109965.

(12) Huo, Z.-Y.; Kim, Y.; Suh, I.; Lee, D.; Lee, J.; Du, Y.; Wang, S.; Yoon, H.; Kim, S. Triboelectrification induced self-powered microbial disinfection using nanowire-enhanced localized electric field. *Nat. Commun.* **2021**, *12*, No. 3693.

(13) Suh, I.-Y.; Huo, Z.; Jung, J.; Kang, D.; Lee, D.; Kim, Y.; Kim, B.; Jeon, J.; Zhao, P.; Shin, J.; Kim, S.; Kim, S. Highly efficient microbial inactivation enabled by tunneling charges injected through two-dimensional electronics. *Sci. Adv.* **2024**, *10*, No. 18.

(14) Hajra, S.; Panda, S.; Song, S.; Song, H.; Panigrahi, B.; Jeong, S.; Mishra, Y.; Kim, H. Simultaneous Triboelectric and Mechanoluminescence Sensing Toward Self-Powered Applications. *Adv. Sustainable Syst.* **2024**, *8*, No. 2400609.

(15) Wu, M.; Xu, Y.; He, Q.; Sun, P.; Weng, X.; Dong, X. Tribocatalysis of homogeneous material with multi-size granular distribution for degradation of organic pollutants. *J. Colloid Interface Sci.* **2022**, *622*, 602–611.

(16) Fu, C.; Wu, T.; Sun, G.; Yin, G.; Wang, C.; Ran, G.; Song, Q. Dual-defect enhanced piezocatalytic performance of C₃N₅ for multifunctional applications. *Appl. Catal., B* **2023**, *323*, No. 122196.

(17) Dong, X.; Wang, Z.; Berbille, A.; Zhao, X.; Tang, W.; Wang, Z. Investigations on the contact-electro-catalysis under various ultrasonic conditions and using different electrification particles. *Nano Energy* **2022**, *99*, No. 107346.

(18) Zhao, J.; Chen, L.; Luo, W.; Li, H.; Wu, Z.; Xu, Z.; Zhang, Y.; Zhang, H.; Yuan, G.; Gao, J.; Jia, Y. Strong tribo-catalysis of zinc oxide nanorods via triboelectrically-harvesting friction energy. *Ceram. Int.* **2020**, *46*, 25293–25298.

(19) He, J.; Zhai, W.; Wang, S.; Wang, Y.; Li, W.; He, G.; Hou, X.; Liu, J.; He, Q. Persistently high Cr⁶⁺ removal rate of centi-sized iron turning owing to tribocatalysis. *Mater. Today Phys.* **2021**, *19*, No. 100408.

(20) Korzeniowski, S.; Buck, R.; Newkold, R.; Kassmi, A.; Laganis, E.; Matsuoka, Y.; Dinelli, B.; Beauchet, S.; Adamsky, F.; Weilandt, K.; Soni, V.; Kapoor, D.; Gunasekar, P.; Malvasi, M.; Brinati, M.; Musio, S. A critical review of the application of polymer of low concern regulatory criteria to fluoropolymers II: Fluoroplastics and fluoroelastomers. *Integr. Environ. Assess. Manage.* **2023**, *19*, 326–354.

(21) Prakash, O.; Tiwari, S.; Maiti, P. Fluoropolymers and their nanohybrids as energy Materials: application to fuel cells and energy harvesting. *ACS Omega* **2022**, *7*, 34718–34740.

(22) Wang, Y.; Zhang, J.; Zhang, W.; Yao, J.; Liu, J.; He, H.; Gu, C.; Gao, G.; Jin, X. Electrostatic field in contact-electro-catalysis driven

C–F bond cleavage of perfluoroalkyl substances. *Angew. Chem., Int. Ed.* **2024**, *63*, No. e202402440.

(23) Wang, Y.; Wei, P.; Shen, Z.; Wang, C.; Ding, J.; Zhang, W.; Jin, X.; Vecitis, C.; Gao, G. O₂-independent H₂O₂ production via water–polymer contact electrification. *Environ. Sci. Technol.* **2024**, *58*, 925–934.

(24) Song, W.-Z.; Zhang, M.; Qiu, H.; Li, C.; Chen, T.; Jiang, L.; Yu, M.; Ramakrishna, S.; Wang, Z.; Long, Z. Insulator polymers achieve efficient catalysis under visible light due to contact electrification. *Water Res.* **2022**, *226*, No. 119242.

(25) Zhang, M.; Song, W.; Chen, T.; Sun, D.; Zhang, D.; Li, C.; Li, R.; Zhang, J.; Ramakrishna, S.; Long, Y. Rotation-mode liquid-solid triboelectric nanogenerator for efficient contact-electro-catalysis and adsorption. *Nano Energy* **2023**, *110*, No. 108329.

(26) Wang, Y.; Xu, Y.; Dong, S.; Wang, P.; Chen, W.; Lu, Z.; Ye, D.; Pan, B.; Wu, D.; Vecitis, C.; Gao, G. Ultrasonic activation of inert poly(tetrafluoroethylene) enables piezocatalytic generation of reactive oxygen species. *Nat. Commun.* **2021**, *12*, No. 3508.

(27) Wang, Y.; Zhang, J.; Pu, L.; Cao, M.; Dong, S.; Vecitis, C.; Gao, G. Unexpected exfoliation and activity of nano poly(tetrafluoroethylene) particles from magnetic stir bars: Discovery and implication. *Chemosphere* **2022**, *291*, No. 132797.

(28) Huang, H.; Tu, S.; Zeng, C.; Zhang, T.; Reshak, A.; Zhang, Y. Macroscopic polarization Enhancement promoting photo- and piezoelectric-induced charge separation and molecular oxygen activation. *Angew. Chem., Int. Ed.* **2017**, *56*, 11860–11864.

(29) Li, Y.; Zhang, W.; Niu, J.; Chen, Y. Mechanism of photogenerated reactive oxygen species and correlation with the antibacterial properties of engineered metal-oxide nanoparticles. *ACS Nano* **2012**, *6*, 5164–5173.

(30) Zhou, T.; Hu, R.; Wang, L.; Qiu, Y.; Zhang, G.; Deng, Q.; Zhang, H.; Yin, P.; Situ, B.; Zhan, C.; Qin, A.; Tang, B. An AIE-active conjugated polymer with high ROS-generation ability and biocompatibility for efficient photodynamic therapy of bacterial infections. *Angew. Chem., Int. Ed.* **2020**, *59*, 9952–9956.

(31) Yang, B.; Chen, Y.; Shi, J. Reactive oxygen species (ROS)-based nanomedicine. *Chem. Rev.* **2019**, *119*, 4881–4985.

(32) Katsumata, H.; Kaneco, S.; Suzuki, T.; Ohta, K.; Yobiko, Y. Sonochemical degradation of 2,3,7,8-tetrachlorodibenzo-p-dioxins in aqueous solution with Fe(III)/UV system. *Chemosphere* **2007**, *69*, 1261–1266.

(33) Torres, R.; Pétrier, C.; Combet, E.; Moulet, F.; Pulgarin, C. Bisphenol A mineralization by integrated ultrasound-UV-iron (II) Treatment. *Environ. Sci. Technol.* **2007**, *41*, 297–302.

(34) Xu, C.; Zi, Y.; Wang, A.; Zou, H.; Dai, Y.; He, X.; Wang, P.; Wang, Y.; Feng, P.; Li, D.; Wang, Z. On the electron-transfer mechanism in the contact-electrification effect. *Adv. Mater.* **2018**, *30*, No. 1706790.

(35) Xu, Y.; Yin, R.; Zhang, Y.; Zhou, B.; Sun, P.; Dong, X. Unveiling the mechanism of frictional catalysis in water by Bi₁₂TiO₂₀: A charge transfer and contaminant decomposition path study. *Langmuir* **2022**, *38*, 14153–14161.

(36) Ruan, L.; Jia, Y.; Guan, J.; Xue, B.; Huang, S.; Wang, Z.; Fu, Y.; Wu, Z. Tribo-electro-catalytic dye degradation driven by mechanical friction using MOF-derived NiCo₂O₄ double-shelled nanocages. *J. Clean. Prod.* **2022**, *345*, No. 131060.

(37) Wang, Z.; Dong, X.; Li, X.; Feng, Y.; Li, S.; Tang, W.; Wang, Z. A contact-electro-catalysis process for producing reactive oxygen species by ball milling of triboelectric materials. *Nat. Commun.* **2024**, *15*, No. 757.

(38) Shen, S.; Fu, J.; Yi, J.; Ma, L.; Sheng, F.; Li, C.; Wang, T.; Ning, C.; Wang, H.; Dong, K.; Wang, Z. High-efficiency wastewater purification system based on coupled Photoelectric-catalytic action provided by triboelectric nanogenerator. *Nanomicro Lett.* **2021**, *13*, No. 194.